Biochem. J. (2013) **449**, 295–305 (Printed in Great Britain) doi:10.1042/BJ20121240

CFTR mutations altering CFTR fragmentation

Kendra TOSONI*[1], Michelle STOBBART*[1], Diane M. CASSIDY*, Andrea VENERANDO†, Mario A. PAGANO‡, Simão LUZ§, Margarida D. AMARAL§¶, Karl KUNZELMANN‖, Lorenzo A. PINNA†, Carlos M. FARINHA§ and Anil MEHTA*[2]

*Division of Medical Sciences, University of Dundee, Ninewells Hospital, Dundee DD1 9SY, U.K., †Department of Biomedical Sciences and CNR Institute of Neurosciences, University of Padova, Viale G. Colombo 3, 35131 Padua, Italy, ‡Department of Molecular Medicine, University of Padova, via U. Bassi 58/B, 35121 Padova, Italy, §University of Lisbon, Faculty of Sciences, BioFIG-Center for Biodiversity, Functional and Integrative Genomics, 1749-016 Lisbon, Portugal, ¶National Institute of Health, Department of Human Genetics, 1649-016 Lisbon, Portugal, and ‖Institut für Physiologie, Universität Regensburg, Universitätsstraße 31, D-93053 Regensburg, Germany

Most CF (cystic fibrosis) results from deletion of a phenylalanine (F^{508}) in the CFTR {CF transmembrane-conductance regulator; ABCC7 [ABC (ATP-binding cassette) sub-family C member 7]} which causes ER (endoplasmic reticulum) degradation of the mutant. Using stably CFTR-expressing BHK (baby-hamster kidney) cell lines we demonstrated that wild-type CTFR and the F508delCFTR mutant are cleaved into differently sized N- and C-terminal-bearing fragments, with each hemi-CFTR carrying its nearest NBD (nucleotide-binding domain), reflecting differential cleavage through the central CFTR R-domain. Similar NBD1-bearing fragments are present in the natively expressing HBE (human bronchial epithelial) cell line. We also observe multiple smaller fragments of different sizes in BHK cells, particularly after F508del mutation (ladder pattern). Trapping wild-type CFTR in the ER did not generate a F508del fragmentation fingerprint. Fragments change their size/pattern again post-mutation at sites involved in CFTR's *in vitro* interaction with the pleiotropic protein kinase CK2 (S511A in NBD1). The F508del and S511A mutations generate different fragmentation fingerprints that are each unlike the wild-type; yet, both mutants generate new N-terminal-bearing CFTR fragments that are not observed with other CK2-related mutations (S511D, S422A/D and T1471A/D). We conclude that the F508delCFTR mutant is not degraded completely and there exists a relationship between CFTR's fragmentation fingerprint and the CFTR sequence through putative CK2-interactive sites that lie near F508.

Key words: casein kinase 2 (CK2), cystic fibrosis, cystic fibrosis transmembrane-conductance regulator (CFTR), fragmentation, ΔF508-CFTR mutation, F508delCFTR.

INTRODUCTION

Most CF (cystic fibrosis) is caused by an in-frame deletion of phenylalanine residue 508 (F^{508}) in an ion channel, CFTR (CF transmembrane-conductance regulator) [1]. This is by far the most common mutation (70–90 % of patients) encoding an F508delCFTR protein that is rerouted from the ER (endoplasmic reticulum) for proteasomal destruction [2,3]. Hence it is believed that restoring mutated channel maturation and or function will improve patient health [3]. However, much uncertainty exists about the mechanistic links between CFTR mutation and the pleiotropic nature of the resultant multi-organ CF disease [4] because F508delCFTR generates apparently unconnected phenotypes such as channelopathies [5], dysfunctional pathogen sensing [6] and frustrated autophagy [7,8]. Unfortunately, this list is not exhaustive [3]. For example, a failure to resolve inflammation is central to premature pulmonary destruction in CF and wt (wild-type)-CFTR restores the set point of inflammation, even in the absence of pathogens, as evidenced by *in vitro* and *in vivo* studies ([9] and references therein). CFTR is alternatively named ABCC7 [ABC (ATP-binding cassette) sub-family C member 7], a family of proteins which utilize the energy of ATP hydrolysis to actively transport substrates across cell membranes [10]. Unfortunately such familial designation does not help clarify matters as no pumped substrate is reported for CFTR [11]. Hence, the original appellation 'Regulator' to the channel by J. Riordan and colleagues in 1989 [12] remains apt, but exactly how and what CFTR regulates remains an enigma more than two decades after the discovery of the defective protein.

To generate its pleiotropic effects, CFTR does not act alone [3,13]. Although conforming to the classical ABC protein structure of two transmembrane domains and two cytosolic NBDs (nucleotide-binding domains) (NBD1 and NBD2), unlike all other ABC family members, CFTR has an additional multiply phosphorylated and unstructured cytosolic R-domain contiguous with the end of NBD1 [1] that is interactive with heterologous protein partners and internal domains of CFTR. There also exists a cytoskeletal CFTR neighbourhood that approximates a number of partnering proteins including N-terminally bound regulators of membrane traffic and C-terminally linked cytoskeletal anchors and their regulators, principally linked to CFTR turnover [13]. CFTR synthesis, processing and destruction are all complex processes [3,14,15] and a recent review suggest that CFTR binds multiple proteins, perhaps at different times and in different cellular locations creating a plasticity of interactions [16]. Protein kinases controlled by second messengers are established CFTR regulators [5,17], but one CFTR-interactive kinase, protein kinase CK2 (formerly casein kinase 2), is an apparently unregulated signalling molecule [18] controlling hundreds of reported targets [19]. In this context, we previously reported that a small peptide fragment of CFTR corresponding to the amino acid sequence straddling the site of the common CFTR mutation at F^{508} (PGTIKENIIF^{508}GVSYDEYR) controls *in vitro* CK2 function [20,21]. This idea was grounded on previous work [22] where

Abbreviations used: ABC, ATP-binding cassette; BHK, baby-hamster kidney; CF, cystic fibrosis; CFTR, CF transmembrane-conductance regulator; ER, endoplasmic reticulum; EV, empty vector; HBE, human bronchial epithelial; HRP, horseradish peroxidase; LDH, lactate dehydrogenase; NBD, nucleotide-binding domain; wt/WT, wild-type.

[1] These authors contributed equally to this work.

[2] To whom correspondence should be addressed (email a.mehta@dundee.ac.uk).

Table 1 The range of anti-CFTR antibodies tested

IP, immunoprecipitation; N/A, not applicable; WB, Western blot.

Antibody	Supplier	Epitope (amino acids in CFTR sequence)	Application	Dilution used for Western blotting
596	CF Foundation	NBD2 (1204–1211)	WB/IP	1:3000
10B6.2	CF Foundation	NBD1 (399–408)	WB/IP	1:500
M3A7	Santa Cruz Biotechnology	C-terminus (1370–1380)	WB	1:500
24-1	R&D Systems	C-terminus (1377–1480)	IP	N/A
MM13-4	Millipore	N-terminus (25–35)	WB/IP	1:500
450	CF Foundation	R-domain (696–705)	WB	1:500
570	CF Foundation	R-domain (731–742)	WB	1:1000
432	CF Foundation	R-domain (762–770)	WB	1:500
217	CF Foundation	R-domain (807–819)	WB	1:1000

we injected this peptide into cells expressing wt- or F508del-CFTR, finding that this peptide only attenuated wt-CFTR channel function by over 50 % provided F^{508} was present in the sequence [22]. Thus a peptide derived from the site of the most common mutation in CFTR was controlling CFTR itself, F^{508}-dependently, through a feedback loop. Separately we observed that intrapeptide substitution of some of the amino acids straddling F^{508} (such as S^{511} and D^{513}), F^{508}-dependently changed CK2 activity [20,21] by differentially regulating CK2's ability to stoichiometrically phosphorylate both itself and some classical CK2 targets. Furthermore, intrapeptide F^{508} deletion alone differentially altered the potency of CK2 action towards its different classes of cellular targets. Thus this CFTR sequence could control both the channel (feed-forward effect, in cell) and an apparently unregulated and pleiotropic protein kinase (feedback effect, *in vitro*).

Given that CFTR is a doubly ATP- and phosphorylation-regulated ion channel [5] manifesting allosteric control [23], our critical result [20,21] was that these allosteric peptide effects towards CK2 function became complexly allosteric as the ATP concentration increased, creating the first ever report of such regulation of this pleiotropic kinase that controls almost every aspect of cell function [19]. To cement the CFTR, F^{508} and CK2 relationship as potentially explanatory of the many unrelated defects found in CF cells, we recently demonstrated that the phospho-proteome of cellular CK2 targets is altered in cells expressing F508delCFTR compared with wt-CFTR [24]. We found that some CK2 substrates were excessively phosphorylated, whereas others incorporated less phosphate than expected. Hence, to collapse these ideas into a single model, it must first be demonstrated that CFTR fragments, that are predicted to be derived from NBD1 (where F^{508} is located), can exist 'in cell'. In the present study we describe the fingerprint of fragmented CFTR in a well-characterized BHK (baby-hamster kidney) cell model [25]. We show how the fingerprint changes first, after deletion of F^{508} and secondly, after mutation of CFTR residues that our *in vitro* data demonstrate to be potential sites for CK2–CFTR interaction (T^{1471}, S^{511} and S^{422} in wt-CFTR) because these CFTR residues are potentially relevant to feedback towards CK2 activity, CFTR turnover or channel function [25]. Our data suggest that wt-CFTR can be cleaved through its R-domain with a fingerprint that is very different after F^{508} deletion, but changes once again after S^{511} or T^{1471} mutation.

MATERIALS AND METHODS

Antibodies

The anti-CFTR antibodies are summarized in Table 1 as described on the CF Foundation Therapeutic website (http://www.cff.org). The anti-β-actin (A5441) and α-tubulin (T5168) antibodies were from Sigma–Aldrich, anti-LDH (lactate dehydrogenase) (sc-33781) was from Santa Cruz Biotechnology. The anti-α-CK2 antibodies were an in-house preparation or kindly provided by Dr D.W. Litchfield (University of Western Ontario, London, ON, Canada). The HRP (horseradish peroxidase)-conjugated secondary antibodies goat anti-rabbit, rabbit anti-mouse HRP and goat anti-mouse HRP were supplied by Dako.

Cell culture, lysis, protein solubilization and Western blotting

The cell culture methods to create the stable CFTR-expressing cell lines (WT, ΔF, WT S422A, WT S422D, WT S511A, WT S511D, WT T1471A and WT T1471D) and their culture protocols have been described recently [25]. The same method was used to create an empty pNUT vector control cell line [EV (empty vector)] to complete the BHK CFTR cell panel. Cells were in growth phase at ~80 % confluence and cell lysis was performed using the following protocol unless specified in the Figure legend. Cells were washed with ice-cold PBS, scraped from the plates, pelleted by centrifugation (800 ***g*** for 5 min at 22 °C) and lysed by the addition of ice-cold buffer consisting of 1 % (v/v) Nonidet P40, 50 mM Tris/HCl (pH 7.5) and 150 mM NaCl with fresh protease inhibitor cocktail (Calbiochem). Cells were lysed by incubation on ice for 20 min and then the lysates were cleared by centrifugation at 17 000 ***g*** for 15 min at 4 °C. The supernatant was collected and subjected to the Bradford assay for protein concentration quantification. HBE (human bronchial epithelial) cells were cultured as described previously [22].

To allow the determination of the various CFTR breakdown products by Western blot analysis, a modified sample buffer was required as advised by Professor R. Frizzell (University of Pittsburgh, Pittsburgh, PA, U.S.A.) and Professor J. Riordan (University of North Carolina at Chapel Hill, Chapel Hill, NC, U.S.A.). This modified Laemmli sample buffer contained DTT (dithiothreitol; 105 mM final concentration) instead of 2-mercaptoethanol to enhance the solubilization of CFTR. For electrophoresis, 4–12 % precast NuPage® Bis-Tris gradient gels were resolved using Mops buffer according to the manufacturer's instructions (Invitrogen). Proteins were transferred on to Optitran BA-S 83 reinforced nitrocellulose membranes (Whatman) with a semi-dry blotter (Biometra) for 1 h at 150 mA.

Membranes were blocked for 1 h in 5 % skimmed milk in TBS-T. Tween 20 (Sigma–Aldrich) was used at 0.2 % in all stages to reduce non-specific signal in the EV samples. Primary antibodies were diluted as shown in Table 1 in 5 % BSA

(Sigma–Aldrich) in TBS-T. Membranes were developed by enhanced chemiluminescence (Pierce).

Immunoprecipitation

For the immunoprecipitation we initially used Bio-Adembeads PAG (Ademtech) as suggested by Dr Piero Pucci (CEINGE-Advanced Biotechnology, Naples, Italy) or Pierce Protein A/G magnetic beads. Since we were seeking full-length CFTR and its fragments, to avoid an antibody entering the gels this system has the advantage that the antibody-to-bead covalent cross-linking protocol is much more efficient when coupled to magnetic pull down than conventional Protein A/G–Sepharose beads. For some experiments, where we wanted to look for as many 'domain-sensitive' pools of CFTR as possible from our lysate, we developed an empirical '4-CFTR-mix' approach. Separate cross-linking of four different CFTR antibodies, each directed against the different domains of CFTR [N-terminus (MM13-4), NBD1 (10B6.2), NBD2 (596) and C-term (24-1)] to separate batches of magnetic beads was performed according to the manufacturer's instructions. Input lysate (500 μg) was incubated with a total of 0.5 μg of each of the different bead-linked antibodies which permitted replicate experiments for each aliquot to allow optimization. Pellets were washed twice with lysis buffer and proteins were eluted directly in sample buffer and loaded on to the gel without beads. This gave reproducible results for our experiments while also permitting individual unmixed bead-cross-linked antibodies to be used when required. The blots were not stripped and re-probed and in the Figures black lines as lane spacers indicate that the lanes have been re-ordered from the same gel to aid clarity; white spaces between lanes reflect separate gels/blots necessitated by using different antibodies.

RESULTS

The fragmentation fingerprint of wt-CFTR

Full-length wt-CFTR was present at ~160–170 kDa, whereas F508delCFTR (ΔF in Figures) was present slightly below at ~150–160 kDa (Figure 1C). First, we searched for wt-CFTR fragments. Using antibodies directed against the two NBDs showed that both NBDs also exist independently of their respective full-length parental CFTR as differently sized fragments (Figures 1A and 1B). The NBD2-bearing fragments (Figure 1A, lane 2) were present at a greater mass than their NBD1-bearing equivalents (Figure 1B, lane 2) suggesting that wt-CFTR is cleaved between the NBDs. The NBD2-bearing fragments were present as a smear of at least two bands with further examples shown in Figures 2(A) and 3, lanes 2 and 5. Thus cleavage creates two discrete sets of large fragments of ~70–100 kDa (bearing NBD2, not NBD1) and ~60 kDa (quadruplet Q1–Q4, bearing NBD1 and not NBD2). Their relatively large masses suggested that they each carried other domains of CFTR. This was confirmed using N- and C-terminal-directed anti-CFTR antibodies (see Figure 1F). We observed similar N-terminal and NBD1 fragments (compare lanes 2 and 3 in Figure 1B) that also run as a quadruplet (Q1–Q4) straddling the 60 kDa marker. In contrast, with respect to more C-terminal domains, a number of closely spaced bands containing NBD2 mostly colocate with the C-terminus (70–100 kDa; Figure 1A, lanes 2 and 3). Given their large size, it is probable that both the NBD1- and NBD2-bearing fragments also contain their cognate transmembrane domains; this was not explored further, but we note that others have found that such domains are relatively resistant to proteolytic degradation [14]. One smaller NBD2-selective fragment exists as a single sharp band at 55 kDa (Figure 1C, lane 2) that is not detected by the anti-NBD1 antibody (lane 5). Independent examples are shown in Figure 2 (compare lanes 2 and 5 with lane 8, and results not shown). To test whether such fragments were artefacts of sample processing, parallel plates of cells were lysed either into a different buffer (see the Figure 2 legend) or directly on the culture dish into our modified SDS/PAGE sample buffer. We observed similar sized large CFTR fragments (compare lanes 5 and 8 in Figure 2A with their equivalents in Figures 1A and 1B using NBD1- and NBD2-directed antibodies). The combined data suggest that wt-CFTR can be cleaved asymmetrically, but almost in half, probably through the R-domain that lies between the NBDs. Cleavage creates multiple large fragments bearing different N- and C-terminal domains, each bearing the nearest NBD in the CFTR sequence. The BHK model system, while useful in revealing the steady-state fingerprint of fragmented CFTR, might not be reflective of the situation in epithelia where the CFTR expression level is much lower. Therefore we tested the pattern of CFTR fragmentation using the HBE airway cell line (Figure 2B) that expresses wt-CFTR from its natural promoter. After prolonged exposure (Figure 2B, b) similar sized large CFTR fragments and faint NBD1-reactive bands were observed (~60 kDa) that became enriched in the region of the NBD1-bearing Q1–Q4 quadruplet at ~60 kDa after immunoprecipitation (Figure 2C, lane 5). Thus our observed fingerprints are unlikely to be a selective consequence of the higher expression levels in the BHK background (see the Discussion section).

The fragmentation fingerprint of F508delCFTR differs from wt CFTR

Compared with wt-CFTR-expressing cells the steady-state F508delCFTR fragmentation fingerprint is very different, irrespective of the method of cell lysis (Figure 1C, lanes 3 and 6, and Figure 2A, lanes 3, 6 and 9) as might have been predicted for this poorly processed and mostly ER-retained mutant that is targeted for degradation [3]. The degradation pathway differs in that the F508del-NBD1 fingerprint (Figures 1D and 1E) is devoid of the wt Q1–Q4 quartet straddling 60 kDa. For this F508del mutant, the NBD1-directed antibody reveals a cluster of closely spaced bands at ~60–70 kDa accompanied by a ladder of smaller fragments observed below ~60 kDa, especially when using the antibody against the N-terminus of F508delCFTR (Figure 1D, lanes 4 and 5). The combined data, together with the prominent ladder bearing F508del-NBD1 is shown in Figure 2(A) when the cells were lysed immediately into SDS/PAGE buffer (lane 9), is consistent with the cellular generation of different sizes of fragmentation products after F^{508} deletion in CFTR.

The blots shown were mostly from different exposures using actin or tubulin as loading controls. To avoid false negatives in fragment detection (e.g. Figure 1C, lane 6), we increased the quantity of lysate loaded to compensate for the low abundance of both this mutant and its fragments (Figure 1E). Despite loading as much as four times more mutant lysate (lane 6), once again no Q1–Q4 quadruplet bearing NBD1 was seen and the ladder pattern of NBD1 fragmentation was seen only at the highest loads together with higher-molecular-mass species running just below the full-length F508delCFTR (lanes 5 and 6, ~110 kDa). Thus F508delCFTR ladders into many different sized NBD1- (plus the N-terminal) bearing fragments with a loss of the prominence of Q1–Q4. For example compare Figure 1(B) (lanes 2 and 3) with Figure 1(D) (lanes 4 and 5) and Figure 1(E). However, this is not the only difference. Even though the F508del mutation in NBD1 lies remotely from NBD2, the expected wt band bearing NBD2- (and C-terminus) at ~70–100 kDa (Figure 1C, lane 2) is now not observed in F508delCFTR-expressing cells, being

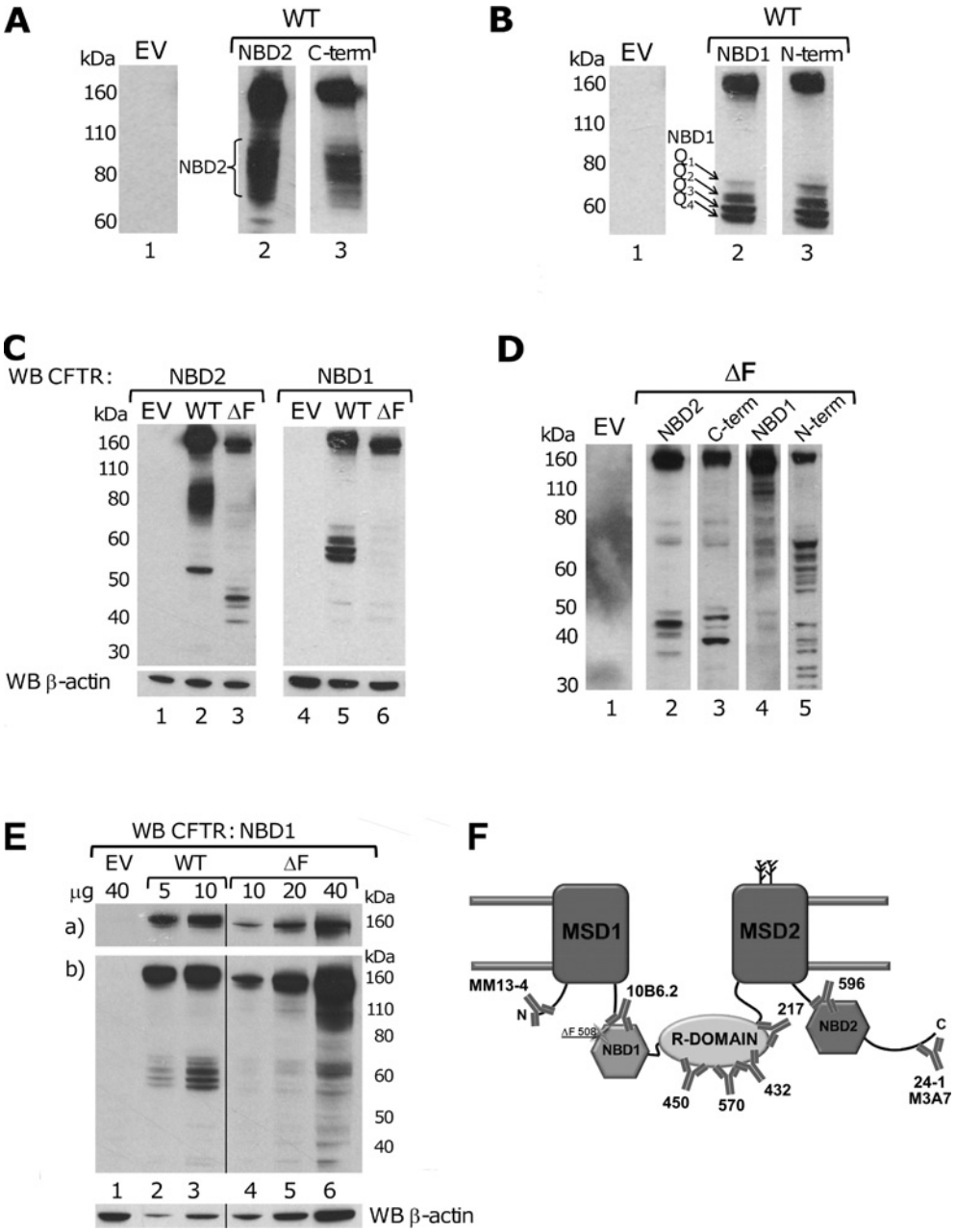

Figure 1 CFTR fragmentation differs between WT and F508delCFTR (ΔF)

The Western blots (**A**–**E**) are derived from stably CFTR-expressing BHK cell lysates. Each is representative of three to six independent experiments from lysates probed with different anti-CFTR antibodies (**F**) directed against CFTR domains [596 (NBD2), M3A7 (C-term), 10B6.2 (NBD1) and MM13-4 (N-term)]. Hemi-fracture of wt-CFTR occurs that separates NBD1- from NBD2- reactive bands. Q refers to a characteristic quartet of bands bearing wt NBD1, the bracket indicates the classic NBD2 fragmentation pattern. (**A**) and (**B**) show examples of 10 or 20 μg protein loads (depending on the antibody efficiency) from the WT BHK lysate. The pNUT vector-alone control cell line (EV) lysates were negative controls. Actin was used as a loading control in this and subsequent Figures unless otherwise stated. Lysates of cells bearing the EV have no non-specific bands even after prolonged exposure (compare EV lanes in **A**–**C** with **D**, lane 1) to a range of anti-CFTR antibodies (Table 1). (**C**) EV, WT and ΔF BHK lysates were analysed by anti-CFTR Western blotting (10 μg input for the NDB2-directed antibody and 20 μg for NBD1). Due to the low expression level, the fragmented bands in F508delCFTR cells are mostly visible in overexposed conditions. (**D**) Examples in which 10–40 μg of proteins from ΔF BHK were analysed to detect fragments of low abundance. (**E**) The blots shown illustrate that the quantity of WT protein that is sufficient to display the fragments is insufficient to display the ΔF fragments unless the latter was severalfold elevated. (**F**) The antibodies as a schematic diagram of Table 1 and Figure 4. For (**A**–**D**) and (**E**) the molecular masses in kDa are given on the left- and right-hand side respectively. WB, Western blot.

replaced by four smaller fragments ranging between 35 kDa and 50 kDa (Figure 1D, lanes 2 and 3), but also accompanied by a number of fainter bands (Figure 2A, lane 6). Thus the F508delCFTR fragmentation fingerprint manifests as a ladder pattern and also displays a greatly fragmented cognate NBD2 (also see the immunoprecipitation data in Figure 3, lanes 3 and 6).

Optimizing the detection of CFTR fragments and the cleavage point in full-length CFTR

Next, using the pooled panel of antibodies spanning the CFTR sequence (see the Materials and methods section for composition and Figure 1F), we immunoprecipitated wt-CFTR

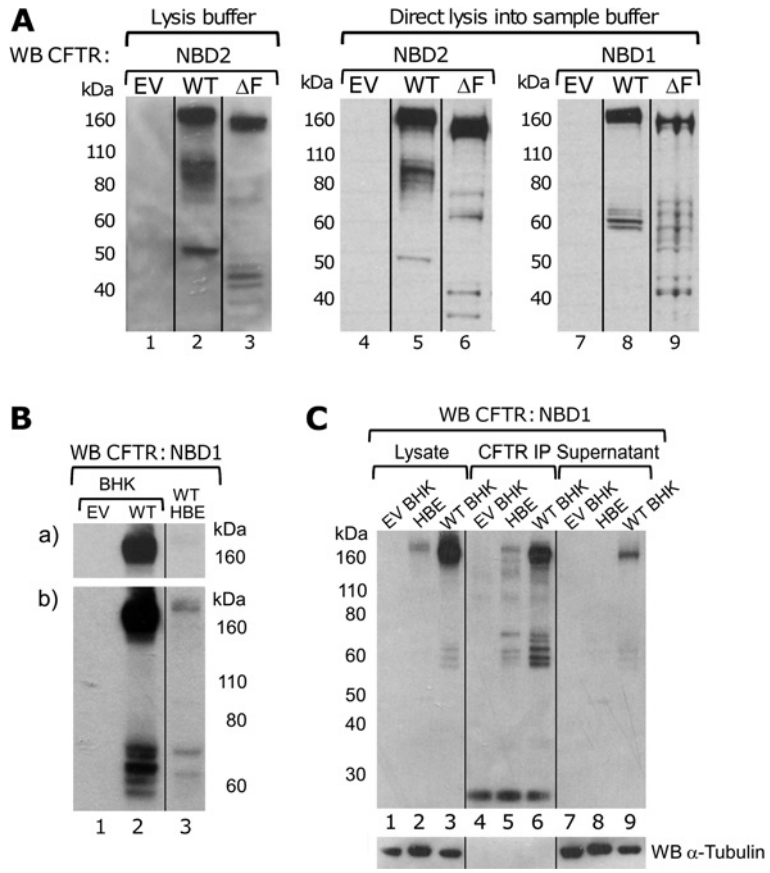

Figure 2 CFTR fragments are not an artefact of cell lysis or cell type

(**A**) Similar NBD2 and NBD1 fractured bands are present when cells are scraped and lysed into a different lysis buffer [0.5 % Triton X-100 and 20 mM Tris/HCl (pH 7.5) and 2 mM EDTA, 2 mM EGTA and 150 mM NaCl] or directly lysed by the addition of the loading buffer for SDS/PAGE 'on plate'. (**B**) Comparing fracture of NBD1 after low CFTR expression in HBE cells. The faint NBD1 fragments (lane 3) are visible. (**C**) The faint NBD1 fragments of CFTR are enriched by immunoprecipitation (lane 5). CFTR was immunoprecipitated using the mixed four antibody approach (0.5 μg of each antibody individually cross-linked to magnetic beads as described in the Material and methods section) at a lysate protein loading of 200 μg for HBE/EV and 100 μg for WT. CFTR content in the input lysate (lanes 1–3: 20 μg for the HBE/EV and 10 μg for WT) was also compared with equal amounts of proteins in the supernatants after the IP (lanes 7–9). IP, immunoprecipitation.

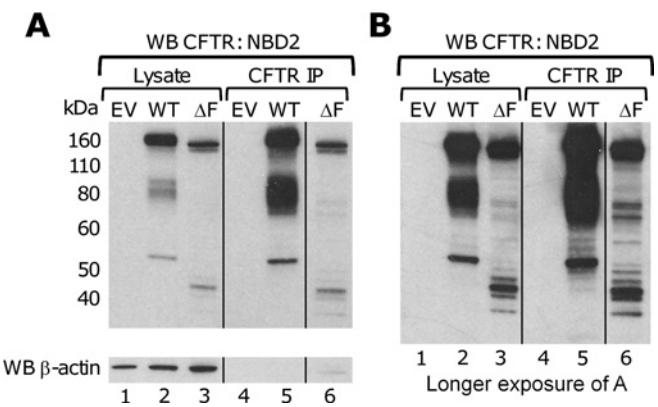

Figure 3 CFTR fragments are present in CFTR immunoprecipitates

CFTR was immunoprecipitated from 500 μg of lysate mixing 2 μg of each antibody cross-linked to beads as described in the Materials and methods section. (**A**) An aliquot of the immunoprecipitate (IP) was analysed in comparison with 10 μg of input lysate by Western blotting (WB) using an anti-NBD2 antibody. The molecular mass in kDa is shown on the left-hand side. (**B**) The longer exposure avoids a false-negative failure to see fragments especially in the F508delCFTR (ΔF) lanes.

and F508delCFTR to determine whether the above fragments were also present. A representative result is shown in Figure 3 (longer exposure in Figure 3B) unequivocally demonstrating that the fragmentation pattern is very different between wt and mutant CFTR for NBD2 (compare lanes 5 and 6 in Figure 3B), but similar to each respective input lysate as shown in lanes 2 and 3. We repeatedly found that the low (relative to the wt) abundance of full-length F508delCFTR leads to a false-negative 'failure' to find fragments at an exposure/input material content capable of detecting the full-length mutant protein (clearly demonstrated in Figure 1E, lane 4). We found that, depending on the antibody used to reliably detect less abundant fragments, at least 20–40 μg (depending on the antibody efficiency) of protein lysate per lane minimized false negatives. For example, compare the apparent absence of the 55 kDa NBD2 fragment in Figure 4(A) lane 17 with its detection at the higher protein loading in lanes 2 in each of Figures 1(C) or Figures 2(A) and 3. Thus, either gross overexposure of the film or a compensatory fold-elevation of mutant input protein lysate, Figure 1(E), is needed to reliably detect CFTR fragments. The immunoprecipitation data from wt-CFTR-expressing cells also confirm that it is possible to immuno-enrich the diffuse NBD2-containing bands at $\sim$80 kDa (compare lanes 2 and 5 in Figure 3), with a characteristic discrete NBD2-reactive singlet that runs at approximately 55 kDa. In contrast the F508delCFTR mutant does not display this cleavage pattern. Instead the F508delCFTR-derived NBD2 is multiply fragmented accompanied by many bands of a greater size that are only

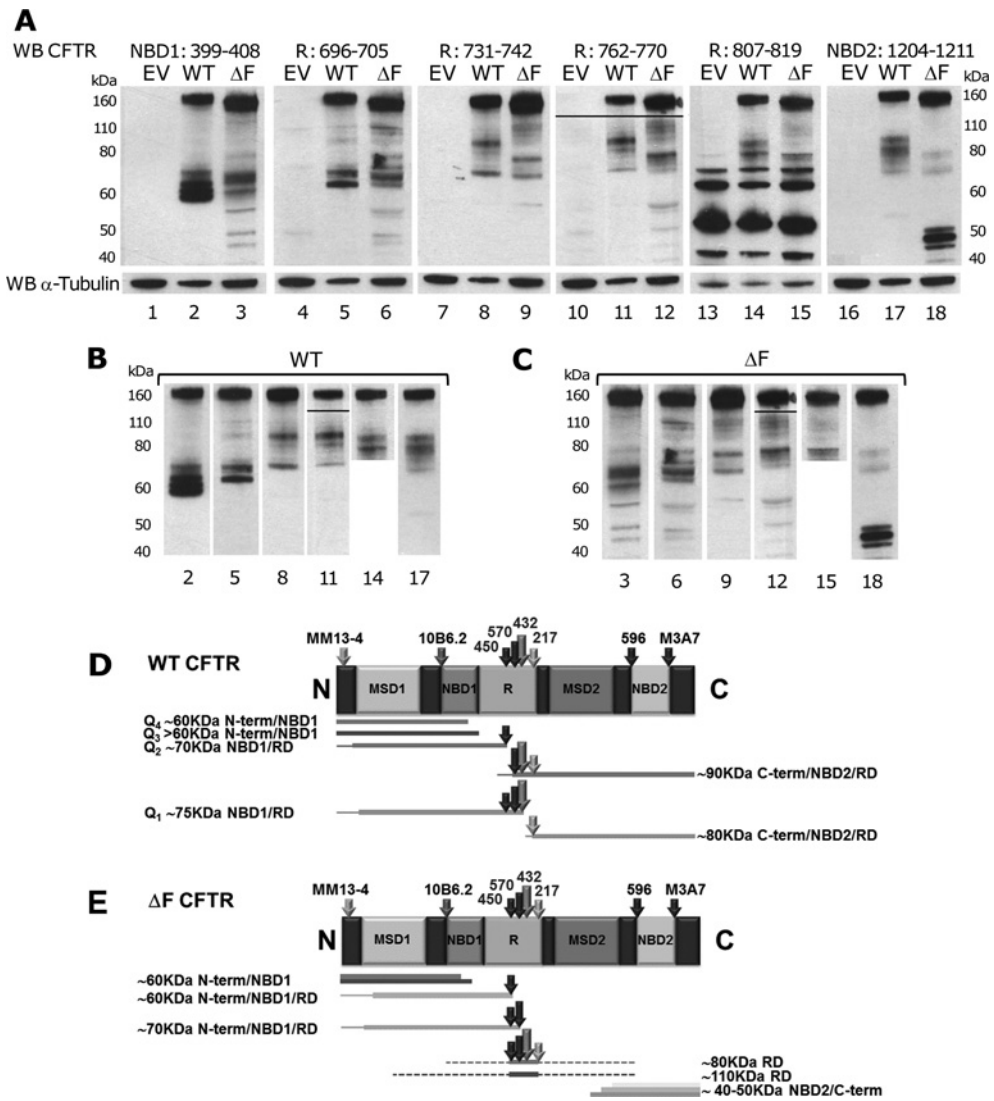

Figure 4 R-domain fragments differ between wt-CTFR and F508delCFTR

BHK lysates were analysed by Western blotting (WB) using antibodies scanned across the R-domain. The blots show the changes in the fingerprint pattern of CFTR fragments (epitopes indicated above the Figures) as the CFTR protein is analysed from NBD1 through the R-domain (R:) towards NBD2. To easily detect fragments at the same exposure the protein load was doubled in ΔF (30 μg, also used for EV) relative to the WT samples (**A**). The lanes are re-ordered in (**B**) and (**C**) to show the step rise in size as the R-domain is traversed towards the C-terminus for the WT (**B**) and the mutant (**C**). The non-specific bands in lanes 14 and 15 should be ignored (compare EV lane 13, omitted from the re-ordered lanes). The cut and splicing (lanes 10–12) compensates for a bubble artefact falsely reducing the level of full-length CFTR (spliced from a re-development of the same gel). α-Tubulin was used as a loading control. Domain composition per fragment is interpreted schematically in (**D**) and (**E**) relating domain detection to CFTR fragment composition and size (RD is R-domain).

detected after overexposure (Figure 3B, overexposed lanes 3 and 6); note the EV (lane 1) remains blank.

We next sought the cleavage point of full-length CFTR (Figure 4), initially characterized as lying within the R-domain that lies between NBD1 and NBD2, but is contiguous with NBD1. Having postulated that CFTR can fracture somewhere between these ATP-binding domains, we probed cell lysates with four different R-domain antibodies. Each antibody was directed against different epitopes spread across the R-domain [antibody numbers 450, 570, 432 and 217 as shown in Figure 1F, respectively raised against: NBD1-adjacent CFTR amino acids 696–705 (lanes 4–6); mid-range R-domain amino acids 731–742 (lanes 7–9) and 762–770 (lanes 10–12); and the least-specific antibody targeting 807–819 which is ∼400 amino acids away from the site recognized by the NBD2 antibody (lanes 13-15); note non-specific bands in EV lane 13]. An important caveat in the use of these antibodies is that only a positive result is informative as implying that the dephosphorylated epitope is present. A negative result does not mean the epitope is absent as it may just be phosphorylated or masked in some other way. Despite this limitation, in each case, R-domain-bearing 'dephospho-fragments' are present (Figure 4A; the corresponding lanes omitting the non-specific bands for ease of comparison are shown in Figures 4B and 4C). An incremental step ladder of R-domain fragment size is seen for wt-CFTR (Figure 4B). The fragments (bearing dephosphorylated serines) increase in mass when scanning across the domain from NBD1 towards NBD2 (Figure 4B, lanes 2, 5, 8, 11, 14 and 17). Bands of the same size as Q1 and Q2 (but not Q3 and Q4) are present when these antibodies are applied. In contrast, the ladder pattern for F508delCFTR, while also demonstrating a step-increment in fragment size as the R-domain is equivalently traversed, also has superimposed an

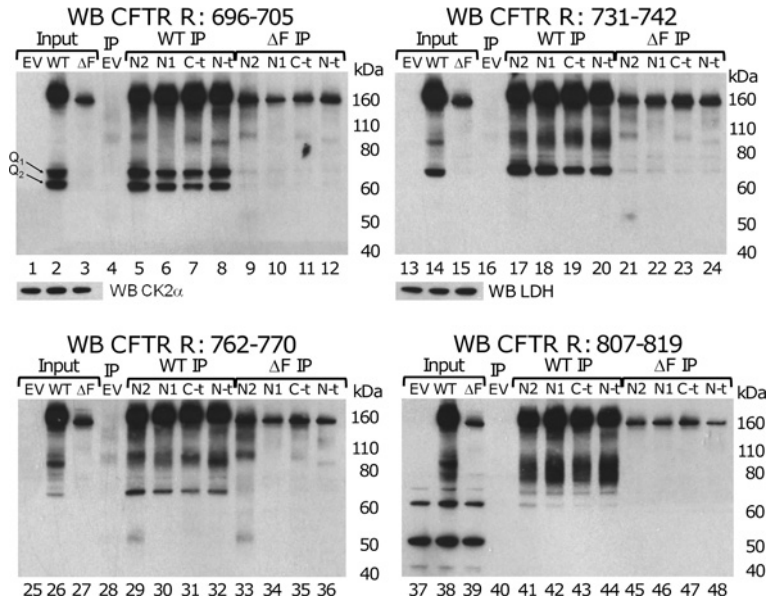

Figure 5 Individual antibodies used to precipitate CFTR followed by R-domain scanning

CFTR was immunoprecipitated (IP) from 250 μg of lysate using 0.5 μg of each antibody cross-linked to beads as described in the Materials and methods section. Aliquots of the immunoprecipitates were analysed in comparison with 10 μg of input lysate by Western blotting (WB) using the indicated antibodies that recognize different regions of the R-domain (RD) of CFTR (see the antibody numbering in Table 1). The fingerprints change as the RD is traversed towards NBD2 suggestive of two cuts. Western blots with anti-CK2α and anti-LDH were used to normalize the inputs [antibodies for immunoprecipitation directed against: NBD1 (N1), NBD2 (N2), C-terminus (Ct) and N-terminus (Nt)]. False-negative failure to find fragments for F508delCFTR is shown on the right-hand side of each blot.

additional pattern displaying fragmented parts of the R-domain, such as the region between 731 and 770 (lane 12) that now appears in smaller fragments (not seen with the 731–742-directed antibody, lane 9) of about 50 kDa. This composite pattern is not seen in the wt R-domain that is found at ~80 kDa (also see Figure 5).

Figure 5 shows the pattern of fragments immunoprecipitated with four different single-bead-linked antibodies directed against either NBD (N2 or N1) or others directed against the extremes of CFTR (C-t or N-t). Each set of precipitated bands is very similar for a given antibody (but not always identical, e.g. scanning across lanes 5–8 shows no 80 kDa band in lane 6). We were surprised to find almost identical domain fragments despite using different domain-directed CFTR antibodies spanning the sequence suggesting that fragments and full-length CFTR are co-located in the same complex. Co-localization is consistent with our unpublished data showing that when we separate membranes from cytosol (by ultracentrifugation), full-length CFTR and fragments remain together. Given the large size of the fragments likely to contain the (fragmentation-resistant) transmembrane domains, future experiments will have to resolve this unexpected association. If it is possible to separate fragments from full-length CFTR we could determine whether or not they are targets for CK2 or if they can act in a regulatory capacity.

As shown for the lysates (Figure 4A), in the immunoprecipitated fragments (Figure 5) the Q1–Q2-sized doublet at 60 kDa disappears as the R-domain is traversed beyond amino acid 705 (lane 14 onwards, compare the fingerprint when amino acids 807–819 are probed). As NBD2 is approached a smear at ~80 kDa increases in intensity. This is best seen in the rearranged data in Figure 6. Combining all of the data from Figures 4 and 5 with fingerprints shown in Figure 6(A) the simplest interpretation is that Q2 is an NBD1-R705 domain-bearing fragment (~60 kDa), whereas Q1 (the band above in Figure 6, ~70 kDa) is a discrete NBD1-R$^{731–770}$-domain-bearing fragment. This is consistent with two different cut sites somewhere between R-domain sites 705 and 731, either from the same parental CFTR species (cut twice) or from different CFTR parents each trimmed discretely (Figure 4D). This fingerprint differs when F508delCFTR is studied (Figure 4E).

Our observed differences in fragmentation post-F^{508} deletion might be explained by the different subcellular compartments in which the wt and mutant CFTR reside because the mutant is thought not to escape from the ER (generating band B, but no band C, Supplementary Figure S1A at http://www.biochemj.org/bj/449/bj4490295add.htm), whereas wt-CFTR transits the ER generating both bands B and C on the Western blots. To investigate the origins of the fragments metabolic pulse labelling was undertaken in BHK cells using a pulse of [^{35}S]methionine to label newly synthesized CFTR as described previously [25]. The hypothesis tested was that newly synthesized CFTR should appear as radiolabelled fragments if fragmented at the same rate as ER synthesis. However, we were unable to detect fragmented CFTR in either the wt or F508delCFTR lysates at a time when full-length radiolabelled CFTR was readily detectable as described previously for this cell line (results not shown). To test the later time points in the synthetic pathway the relatively prolonged ER residence time for F508delCFTR relative to wt- CFTR was exploited. We trapped wt-CFTR in the ER by arresting its onward transfer to the Golgi with Brefeldin A, as described in the Supplementary Online data (at http://www.biochemj.org/bj/449/bj4490295add.htm). This enhanced band B as expected (Supplementary Figure S1A). However, the fragmentation fingerprint of the newly ER-imprisoned wt-CFTR did not now resemble that found with F508delCFTR (Supplementary Figure S1, compare the middle panels). Importantly, for F508delCFTR, Brefeldin A itself induced no change in the fragment signature which remained different from the wt. Thus wt-CFTR, when pharmacologically trapped in the ER, retains its usual fracture fingerprint that remains very different

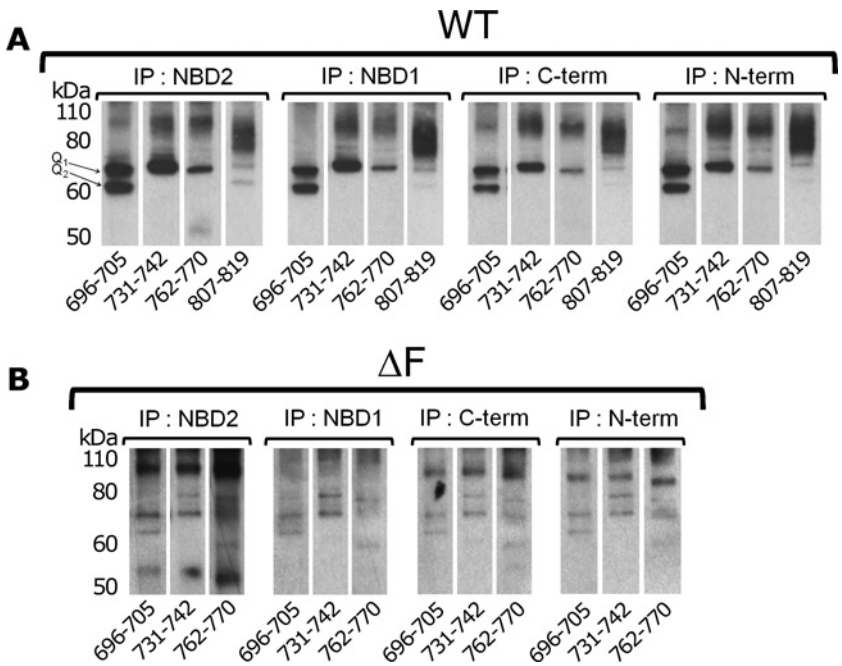

Figure 6 Comparative R-domain fragmentation of WT and F508delCFTR

Data from Figure 5 re-ordered to show that the choice of precipitating antibody does not alter the different patterns of fragmentation as determined by scanning across the CFTR. F508delCFTR fragments differ greatly from the wt as seen in Figures 1 and 2. IP, immunoprecipitation.

from F508delCFTR. Thus we can exclude differential exposure to a proteolytic pathway in the ER as a trivial explanation for the differential fracture fingerprint after F^{508} deletion. This suggests that the sequence of CFTR might itself determine the fragmentation fingerprint.

Fragmentation fingerprints of CFTR mutated at putative CK2-interactive sites

Recently we reported the complex effects on CFTR synthesis, turnover and channel function after mutating three potential CK2 sites in wt-CFTR (S^{422}, S^{511} and T^{1471}) to (non-phosphorylatable) alanine or (phosphomimic) aspartate residues [25]. The most dramatic effect on synthesis was seen after the T1471D mutation (augmenting the negative charge at the regulatory acid stretch, nine amino acids from the C-terminus of wt-CFTR), which abolished the mature 'band C' form of CFTR reminiscent of the findings when F508delCFTR fails to mature in the Golgi from band B (in the ER) to band C (in the plasma membrane). We therefore tested CFTR fragmentation after mutation of the above sites to see if it would change with mutation. Figure 7 shows representative Western blotting data from three independent experiments using the above four CFTR antibodies to scan the mutated CK2 site fragments.

wt-CFTR with mutated S^{422}

When recombinant CK2 was added to NBD1 we found that S^{422} was phosphorylated (see the Introduction). Compared with each other S422D- and S422A-CFTR revealed no gross differences in fragmentation (Figures 7A–7D, compare lanes 3 and 4). Minor differences only manifest as different relative intensities of the Q1–Q4 fragments in NBD1 (Figure 7A). No consistent changes were seen for the NBD2 and C-terminal fragments (Figures 7C and 7D). The difference in intensity of C-terminal CFTR staining relative to wt-CFTR in lane 2 in Figure 7(D) was not explored further given that, in the same cell line, we had also found that mutation of S^{422} had no effect on CFTR synthesis or turnover [25].

wt-CFTR with mutated S^{511}

In sharp contrast, mutation of the S^{511} residue, which is involved in imparting allosteric modulation of CK2 *in vitro*, has dramatic effects on CFTR fragmentation despite never being phosphorylated by CK2 in our studies. The fingerprints differed depending on the domain of CFTR being probed.

S511A-CFTR and its cognate NBD2

The diffuse 80 kDa NBD2 and the C-terminal-bearing fragment so characteristic of the wt-CFTR fingerprint is now grossly attenuated (Figure 7C, compare lanes 2 and 5). However, after blot overexposure, a C-terminal reactive band can be seen in Figure 7(D) (lane 5) suggesting three possibilities. First, the fragment bearing NBD2 and the C-terminus of CFTR may be more easily degraded when the N-terminal 110 kDa (NDB1/N-terminal) fragment (Figures 7A and 7B) is generated by the S511A mutation. Secondly, the epitope of NBD2 recognized by this monoclonal antibody (WPSGGQMT) may be masked after S511A mutation by some post-translational event. Thirdly, the CFTR fracture point induced by this S511A mutant lies near this region as opposed to the R-domain region seen with wt-CFTR in the Figures above.

S511A-CFTR and its cognate NBD1

Consistent with the idea of an altered fracture point when S511A-CFTR is present, a new faint ~100–110 kDa band appears. This is detectable only with the anti-NBD1 and anti-N-terminal

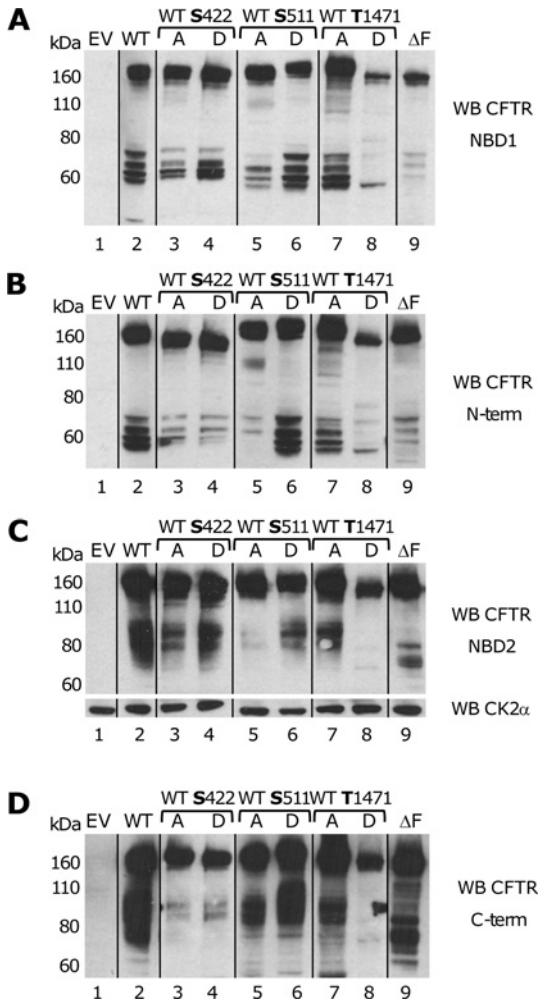

Figure 7 CFTR mutation at two putative CK2 interaction sites alters fragmentation

Common lysate aliquots probed with different antibodies (**A**–**D**) are shown. Note the N-terminal- and NBD1- (but not NBD2) bearing ~120 kDa fragment seen after S511A (but not S511D) mutation in lanes 5 and 6 in (**A**) and (**B**), but not in (**C**) and (**D**), the latter probing the C-terminus. Compare similarities and differences in fragmentation between lanes 8 and 9 which both reduce the amount of full-length CFTR (T1471D or F508del). Molecular masses are shown on the left-hand side in kDa. WB. Western blot.

antibodies (Figure 7, lanes 5, compare between the 110 and 160 kDa markers in 7A and 7B with 7C and 7D) noting that, simultaneously, the quartet Q1–Q4 at 60 kDa, are attenuated in 7(A) (Q1 is faint) and 7(B) (all attenuated, Q3 and Q4, not seen). Attenuation of the quartet, although found in the majority of experiments, was not always present (results not shown). Thus it is probable that the S511A mutation creates a band at 100–110 kDa-bearing NBD1 and the N-terminus, but we cannot be sure about the relationship between this band and the relative amounts of the Q1–Q4 NBD1-bearing fragments.

S511D-CFTR and NBD1 and NBD2

This phosphomimic fingerprint is similar to the wt in fragmentation pattern and no 110 kDa band appears, even after overexposure (Figure 7, lanes 6 and results not shown). The presence or absence of this new ~110 kDa band after mutation of S^{511} is consistent in four independent experiments (results not shown). The combined S^{511} site mutant data suggest the existence of a new S511A-dependent CFTR cleavage whose generation is either dependent on the non-availability of the expected wt hydroxy group on S^{511} or is induced by a structural change after substitution with alanine (but not the negatively charged aspartate).

wt-CFTR with mutated T^{1471}

T1471A fragmentation is very similar to the wt. In contrast T1471D displays gross attenuation of all fragments (only Q4 remains visible with the NBD1 and N-terminal antibodies). The absence of other bands may be a false-negative artefact of low fragment abundance because we find that the full-length wt-CFTR with the T1471D mutation is also attenuated and thus (from an abundance perspective) is indistinguishable from the pattern seen with F508delCFTR, despite the wt background. This confirms recent data [25] showing that T1471D abolished the formation of any fully glycosylated band C CFTR in the same cell line and is consistent with the importance of the acid cluster surrounding T^{1471} towards the relative rates of opening and closing of CFTR [26]. T^{1471} provides an excellent CK2 consensus target embedded within this conserved acid cluster of five surrounding glutamates, whose combined deletion is unexpectedly deleterious to CFTR-dependent ion transport [26].

In summary, the two S511A/S511D and T1471A/T1471D pairs manifested very different CFTR cleavage patterns and abundance of full-length CFTR when present on a wt background. The consistent finding is that fragmentation differed dependening on the type of mutation introduced at S^{511} and T^{1471} (but not S^{422}, with the possible exception of the C-terminus). Overall, this suggests a complex relationship between CFTR fracture pattern and the amino acids located at F^{508}, S^{511} and T^{1471}. Only F508delCFTR and S511A CFTR generated a new CFTR band at about 110 kDa.

DISCUSSION

Previous work suggests that exogenously expressed fragments of CFTR might have therapeutic potential to correct F508delCFTR function [27,28]. The results of the present study demonstrated that cells generate endogenous CFTR fragments whose combined fingerprint differs not only after F^{508} deletion, but also after mutation of residues S^{511} and T^{1471} that are relevant to the regulatory interactions of CFTR with protein kinase CK2 (compare Figures 1 and 7). Differences in CFTR fragmentation patterns (fingerprints) are also present in cells directly solubilized without any intermediate processing (Figure 2A). The observed CFTR fragments create a consistent fingerprint compatible with the reported differential *in vitro* sensitivities towards proteolysis between wt-CTFR and F508delCFTR [14,29]. We also demonstrated that F508delCFTR is not immediately degraded and that the mutant NBD fragments are very different from the wt. The fingerprints of wt-CTFR and F508delCFTR both suggest cleavage through the unstructured and heavily phosphorylated R-domain that lies between the NBDs (Figures 4D and 4E). This hemi-cleavage of CFTR through the R-domain is also observed after deletion of F^{508}, but manifests a superimposed ladder of additional fragments. The observed patterns are unlikely to be a quirk of our chosen cell line because we find similar fragments in a wt-CFTR-expressing airway cell line (Figures 2B and 2C). Mechanistically, differential subcellular compartmental residence time, as occurs with the unfolded F508delCFTR, is an unlikely explanation for the differential fingerprints because pharmacologically ER-trapped wt-CFTR does not display an F508del fracture fingerprint (see the Supplementary Online data).

It is also unlikely that CK2-relevant CFTR mutants such as S511A- and S511D-CFTR generate an ER-trapped unfolded CFTR, as they have wt patterns of maturation and turnover during pulse–chase experiments in the same cell line [25]; yet, they manifest very different fragmentation. Thus maturation and fragmentation may be temporally late events which might explain why we observed no fragments during early pulse–chase experiments to track the fate of nascent CFTR. The simplest interpretation is that CFTR first matures and is then fragmented differently, depending on the internal CFTR sequence near F^{508}, such as S^{511}.

We observe that the fragmentation fingerprints change after either eliminating or mimicking phosphorylation at two CK2 -relevant sites: S^{511}, that lies in NBD1 [32] and T^{1471} in the C-terminus of CFTR (but not S^{422}, an *in vitro* CK2 target in the R-domain). T^{1471} is embedded in a (channel-regulatory) acid-rich region [26] close to the C-terminus, whereas S^{511} lies within a site that interacts *in vitro* with F^{508} to impart regulation towards CK2 targeting and or function [20,21].

While the present study was in progress two publications using native CFTR-expressing cells and other cell lines also showed a novel 100 kDa CFTR, albeit generated by calpain cleavage [30,31,] consistent with the *in vitro* data from another group [33]. The latter reported that, during the *in vitro* addition of recombinant cytoplasmic-facing CFTR domains (bearing NBD1 and R-domain) to cell lysates, cleavage of their CFTR construct also occurred in the R-domain region. Calpains are a family of 'modulator proteases' that create newly functional fracture products [30,34] whose actions overlap with aspartate-directed proteases (caspases) that are linked to CK2 function [35]. For example, CK2-induced phosphorylation can render a potential caspase cleavage target blind to cleavage recognition, but we do not yet know if any CK2 phosphorylation occurs in this region of the R-domain 'in cell' although, as we recently reported [25], CFTR contains several consensus phosphorylation sites for this kinase (S^{605}, S^{629}, S^{678}, T^{803} and T^{816}). We also recently reported that the CK2 phospho-proteome is abnormal in lysates from F508delCFTR-expressing BHK cells [24] consistent with *in vitro* findings that peptides corresponding to the common F^{508} deletion site on CFTR have a many-fold-enhanced effect on the CK2 holoenzyme over their wt equivalents [20,21]. Additionally, CK2 controls CFTR channel function across diverse epithelia including intact excised organs [22,25]. In the present study we add a new finding that deletion of F^{508} or substitution of T^{1471} to a phospho-mimic not only dramatically decrease the quantity, but differentially alters the fragmentation fingerprint of mutated CFTR (Figures 1 and 7, lane 9).

We do not claim that CK2 dysfunction is the sole pathogenic mechanism in CF pathogenesis. Our central argument in linking CK2 miscontrol through F^{508} to CF pathogenesis rests on our inability to explain why a cell, which must cope with a daily flux of thousands of misfolded membrane proteins, can be so profoundly disrupted by its inability to fold F508delCFTR, especially given the high selectivity of the defective turnover of this mutant that appears to be confined to CFTR itself without disrupting either endocytosis or the turnover of an unrelated ABC protein [36]. One possibility is that there exists a latent (knockin) role for this particular F^{508} deletion in the CFTR mutant that prevents its own clearance. This hidden dominant effect is predicted to be present in the heterozygote F508del carrier, i.e. to be found in approximately 1 in 60 healthy Europeans because only this F508del allele (among over 1900 CFTR alleles competing against the wt sequence) shows a relative population-level allelic enrichment at $\sim$500-fold. Hence, F508delCFTR carriers must have accrued a sustained relative advantage in the *cftr* allelic race over millennia which suggests a function for F508delCFTR despite its recessive carriage (and presumed ER destruction). Given the dual importance of the F^{508} region of CFTR [37,38] and CK2 in inflammation and host defence [39], and our recent finding that a tyrosine kinase linked to inflammation [SYK (spleen tyrosine kinase)] also controls CFTR in a CK2-interactive manner near the F^{508} site [25], we have proposed that by adding (CFTR) peptide-induced miscontrol of CK2 to established models of CF pathogenesis, we might illuminate the complex path from the F508delCFTR defect to CF disease [24]. Thus the most pleiotropic protein kinase and an equivalently pleiotropic lethal recessive inherited disease of children could have a hidden relationship. Our claim is that, in CF, among the multitude of (disrupted) pathway possibilities [40–42], a single protein kinase, CK2, stands apart as being the most pleiotropic of all, exerting simultaneous control of many hundreds of substrates across fundamental CF-related cellular processes, while always appearing to be active 'in cell' and yet manifesting lethality when deleted. We contend that a latent CK2–F508delCFTR relationship might just be a regulator of (nearly) everything and one factor in the long sought regulatory role of CFTR across multiple cell pathways.

AUTHOR CONTRIBUTION

Kendra Tosoni and Michelle Stobbart carried out the experimental work with Diane Cassidy. Andrea Venerando and Mario Pagano advised on some of the experiments and revised the paper text and CFTR fracture Figures. Simão Luz, Margarida Amaral and Carlos Farinha made the BHK cells and performed the pulse–chase experiments. Karl Kunzelmann and Lorenzo Pinna discussed the data/design and advised on the experiments. Anil Mehta designed experiments and wrote most of the paper.

FUNDING

This work was supported by the Wellcome Trust [grant numbers 088929 (to L.A.P. and A.M.) and 069150 (to A.M.)], the FCT (Fundação para a Ciência e a Tecnologia) [grant numbers PTDC/BIA-BCM/112635/2009, PEst-OE/BIA/UI4046/2011 and SFRH/BD/47445/2008 (to S.L.)] and the Fondazione per la Ricerca sulla Fibrosi Cistica [grant number 3/2011 (to L.A.P.)].

REFERENCES

1 Riordan, J. R. (2005) Assembly of functional CFTR chloride channels. Annu. Rev. Physiol. **67**, 701–718
2 Gelman, M. S., Kannegaard, E. S. and Kopito, R. R. (2002) A principal role for the proteasome in endoplasmic reticulum-associated degradation of misfolded intracellular cystic fibrosis transmembrane conductance regulator. J. Biol. Chem. **277**, 11709–11714
3 Lukacs, G. L. and Verkman, A. S. (2012) CFTR: folding, misfolding and correcting the ΔF508 conformational defect. Trends Mol. Med. **18**, 81–91
4 Kunzelmann, K. (2001) CFTR: interacting with everything? News Physiol. Sci. **16**, 167–170
5 Sheppard, D. N. and Welsh, M. J. (1999) Structure and function of the CFTR chloride channel. Physiol. Rev. **79**, S23–S45
6 Pier, G. B., Grout, M. and Zaidi, T. S. (1997) Cystic fibrosis transmembrane conductance regulator is an epithelial cell receptor for clearance of *Pseudomonas aeruginosa* from the lung. Proc. Natl. Acad. Sci. U.S.A. **94**, 12088–12093
7 Luciani, A., Villella, V. R., Esposito, S., Brunetti-Pierri, N., Medina, D., Settembre, C., Gavina, M., Pulze, L., Giardino, I., Pettoello-Mantovani, M. et al. (2010) Defective CFTR induces aggresome formation and lung inflammation in cystic fibrosis through ROS-mediated autophagy inhibition. Nat. Cell Biol. **12**, 863–875
8 Luciani, A., Villella, V. R., Esposito, S., Brunetti-Pierri, N., Medina, D. L., Settembre, C., Gavina, M., Raia, V., Ballabio, A. and Maiuri, L. (2011) Cystic fibrosis: a disorder with defective autophagy. Autophagy **7**, 104–106
9 Hunter, M. J., Treharne, K. J., Winter, A. K., Cassidy, D. M., Land, S. and Mehta, A. (2010) Expression of wild-type CFTR suppresses NF-κB-driven inflammatory signalling. PLoS ONE **5**, e11598

10 Holland, I. B. (2011) ABC transporters, mechanisms and biology: an overview. Essays Biochem. **50**, 1–17
11 Riordan, J. R. and Chang, X. B. (1992) CFTR, a channel with the structure of a transporter. Biochim. Biophys. Acta **1101**, 221–222
12 Riordan, J. R., Rommens, J. M., Kerem, B., Alon, N., Rozmahel, R., Grzelczak, Z., Zielenski, J., Lok, S., Plavsic, N., Chou, J. L. et al. (1989) Identification of the cystic fibrosis gene: cloning and characterization of complementary DNA. Science **245**, 1066–1073
13 Li, C. and Naren, A. P. (2010) CFTR chloride channel in the apical compartments: spatiotemporal coupling to its interacting partners. Integr. Biol. **2**, 161–177
14 Kleizen, B., van Vlijmen, T., de Jonge, H. R. and Braakman, I. (2005) Folding of CFTR is predominantly cotranslational. Mol. Cell **20**, 277–287
15 Van Oene, M., Lukacs, G. L. and Rommens, J. M. (2000) Cystic fibrosis mutations lead to carboxyl-terminal fragments that highlight an early biogenesis step of the cystic fibrosis transmembrane conductance regulator. J. Biol. Chem. **275**, 19577–19584
16 Guggino, W. B. and Stanton, B. A. (2006) New insights into cystic fibrosis: molecular switches that regulate CFTR. Nat. Rev. Mol. Cell Biol. **7**, 426–436
17 Kongsuphol, P., Cassidy, D., Hieke, B., Treharne, K. J., Schreiber, R., Mehta, A. and Kunzelmann, K. (2009) Mechanistic insight into control of CFTR by AMPK. J. Biol. Chem. **284**, 5645–5653
18 Pinna, L. A. (1990) Casein kinase 2: an 'eminence grise' in cellular regulation? Biochim. Biophys. Acta **1054**, 267–284
19 Meggio, F. and Pinna, L. A. (2003) One-thousand-and-one substrates of protein kinase CK2? FASEB J. **17**, 349–368
20 Pagano, M. A., Arrigoni, G., Marin, O., Sarno, S., Meggio, F., Treharne, K. J., Mehta, A. and Pinna, L. A. (2008) Modulation of protein kinase CK2 activity by fragments of CFTR encompassing F^{508} may reflect functional links with cystic fibrosis pathogenesis. Biochemistry **47**, 7925–7936
21 Pagano, M. A., Marin, O., Cozza, G., Sarno, S., Meggio, F., Treharne, K. J., Mehta, A. and Pinna, L. A. (2010) Cystic fibrosis transmembrane regulator fragments with the Phe^{508} deletion exert a dual allosteric control over the master kinase CK2. Biochem. J. **426**, 19–29
22 Treharne, K. J., Xu, Z., Chen, J. H., Best, O. G., Cassidy, D. M., Gruenert, D. C., Hegyi, P., Gray, M. A., Sheppard, D. N., Kunzelmann, K. and Mehta, A. (2009) Inhibition of protein kinase CK2 closes the CFTR Cl channel, but has no effect on the cystic fibrosis mutant ΔF508-CFTR. Cell. Physiol. Biochem. **24**, 347–360
23 Kirk, K. L. and Wang, W. (2011) A unified view of cystic fibrosis transmembrane conductance regulator (CFTR) gating: combining the allosterism of a ligand-gated channel with the enzymatic activity of an ATP-binding cassette (ABC) transporter. J. Biol. Chem. **286**, 12813–12819
24 Venerando, A., Pagano, M. A., Tosoni, K., Meggio, F., Cassidy, D., Stobbart, M., Pinna, L. A. and Mehta, A. (2011) Understanding protein kinase CK2 mis-regulation upon F508del CFTR expression. Naunyn Schmiedebergs Arch. Pharmacol. **384**, 473–488
25 Luz, S., Kongsuphol, P., Mendes, A. I., Romeiras, F., Sousa, M., Schreiber, R., Matos, P., Jordan, P., Mehta, A., Amaral, M. D. et al. (2011) Contribution of casein kinase 2 and spleen tyrosine kinase to CFTR trafficking and protein kinase A-induced activity. Mol. Cell. Biol. **31**, 4392–4404
26 Ostedgaard, L. S., Randak, C., Rokhlina, T., Karp, P., Vermeer, D., Ashbourne Excoffon, K. J. and Welsh, M. J. (2003) Effects of C-terminal deletions on cystic fibrosis transmembrane conductance regulator function in cystic fibrosis airway epithelia. Proc. Natl. Acad. Sci. U.S.A. **100**, 1937–1942
27 Dong, Q., Ostedgaard, L. S., Rogers, C., Vermeer, D. W., Zhang, Y. and Welsh, M. J. (2012) Human-mouse cystic fibrosis transmembrane conductance regulator (CFTR) chimeras identify regions that partially rescue CFTR-ΔF508 processing and alter its gating defect. Proc. Natl. Acad. Sci. U.S.A. **109**, 917–922
28 Cormet-Boyaka, E., Hong, J. S., Berdiev, B. K., Fortenberry, J. A., Rennolds, J., Clancy, J. P., Benos, D. J., Boyaka, P. N. and Sorscher, E. J. (2009) A truncated CFTR protein rescues endogenous ΔF508-CFTR and corrects chloride transport in mice. FASEB J. **23**, 3743–3751
29 Zhang, F., Kartner, N. and Lukacs, G. L. (1998) Limited proteolysis as a probe for arrested conformational maturation of ΔF508 CFTR. Nat. Struct. Biol. **5**, 180–183
30 Averna, M., Stifanese, R., Grosso, R., Pedrazzi, M., De Tullio, R., Salamino, F., Pontremoli, S. and Melloni, E. (2010) Role of calpain in the regulation of CFTR (cystic fibrosis transmembrane conductance regulator) turnover. Biochem. J. **430**, 255–263
31 Averna, M., Stifanese, R., Grosso, R., Pedrazzi, M., De Tullio, R., Salamino, F., Sparatore, B., Pontremoli, S. and Melloni, E. (2011) Calpain digestion and HSP90-based chaperone protection modulate the level of plasma membrane F508del-CFTR. Biochim. Biophys. Acta **1813**, 50–59
32 Atwell, S., Brouillette, C. G., Conners, K., Emtage, S., Gheyi, T., Guggino, W. B., Hendle, J., Hunt, J. F., Lewis, H. A., Lu, F. et al. (2010) Structures of a minimal human CFTR first nucleotide-binding domain as a monomer, head-to-tail homodimer, and pathogenic mutant. Protein Eng. Des. Sel. **23**, 375–384
33 Stratford, F. L., Pereira, M. M., Becq, F., McPherson, M. A. and Dormer, R. L. (2003) Benzo(c)quinolizinium drugs inhibit degradation of ΔF508-CFTR cytoplasmic domain. Biochem. Biophys. Res. Commun. **300**, 524–530
34 Stifanese, R., Averna, M., De Tullio, R., Salamino, F., Cantoni, C., Mingari, M. C., Prato, C., Pontremoli, S. and Melloni, E. (2008) Role of the calpain-calpastatin system in the density-dependent growth arrest. Arch. Biochem. Biophys. **479**, 145–152
35 Turowec, J. P., Duncan, J. S., Gloor, G. B. and Litchfield, D. W. (2011) Regulation of caspase pathways by protein kinase CK2: identification of proteins with overlapping CK2 and caspase consensus motifs. Mol. Cell. Biochem. **356**, 159–167
36 Swiatecka-Urban, A., Brown, A., Moreau-Marquis, S., Renuka, J., Coutermarsh, B., Barnaby, R., Karlson, K. H., Flotte, T. R., Fukuda, M., Langford, G. M. and Stanton, B. A. (2005) The short apical membrane half-life of rescued ΔF508-cystic fibrosis transmembrane conductance regulator (CFTR) results from accelerated endocytosis of ΔF508-CFTR in polarized human airway epithelial cells. J. Biol. Chem. **280**, 36762–36772
37 Treharne, K. J., Cassidy, D., Goddard, C., Colledge, W. H., Cassidy, A. and Mehta, A. (2009) Epithelial IgG and its relationship to the loss of F^{508} in the common mutant form of the cystic fibrosis transmembrane conductance regulator. FEBS Lett. **583**, 2493–2499
38 Cohen, J. C., Killeen, E., Chander, A., Takemaru, K., Larson, J. E., Treharne, K. J. and Mehta, A. (2009) Small interfering peptide (siP) for *in vivo* examination of the developing lung interactonome. Dev. Dyn. **238**, 386–393
39 Singh, N. N. and Ramji, D. P. (2008) Protein kinase CK2, an important regulator of the inflammatory response? J. Mol. Med. **86**, 887–897
40 Hosoi, T., Korematsu, K., Horie, N., Suezawa, T., Okuma, Y., Nomura, Y. and Ozawa, K. (2012) Inhibition of casein kinase 2 modulates XBP1-GRP78 arm of unfolded protein responses in cultured glial cells. PLoS ONE **7**, e40144
41 Koch, S., Capaldo, C. T., Hilgarth, R. S., Fournier, B., Parkos, C. A. and Nusrat, A. (2012) Protein kinase CK2 is a critical regulator of epithelial homeostasis in chronic intestinal inflammation. Mucosal Immunol., doi:10.1038/mi.2012.57
42 Watabe, M. and Nakaki, T. (2011) Protein kinase CK2 regulates the formation and clearance of aggresomes in response to stress. J. Cell Sci. **124**, 1519–1532

Received 3 August 2012/2 October 2012; accepted 15 October 2012
Published as BJ Immediate Publication 15 October 2012, doi:10.1042/BJ20121240

Biochem. J. (2013) **449**, 295–305 (Printed in Great Britain) doi:10.1042/BJ20121240

online data

SUPPLEMENTARY ONLINE DATA

CFTR mutations altering CFTR fragmentation

Kendra TOSONI*[1], Michelle STOBBART*[1], Diane M. CASSIDY*, Andrea VENERANDO†, Mario A. PAGANO‡, Simão LUZ§, Margarida D. AMARAL§¶, Karl KUNZELMANN‖, Lorenzo A. PINNA†, Carlos M. FARINHA§ and Anil MEHTA*[2]

*Division of Medical Sciences, University of Dundee, Ninewells Hospital, Dundee DD1 9SY, U.K., †Department of Biomedical Sciences and CNR Institute of Neurosciences, University of Padova, Viale G. Colombo 3, 35131 Padua, Italy, ‡Department of Molecular Medicine, University of Padova, via U. Bassi 58/B, 35121, Padova, Italy, §University of Lisbon, Faculty of Sciences, BioFIG-Center for Biodiversity, Functional and Integrative Genomics, 1749-016 Lisbon, Portugal, ¶National Institute of Health, Department of Human Genetics, 1649-016 Lisbon, Portugal, and ‖Institut für Physiologie, Universität Regensburg, Universitätsstraße 31, D-93053 Regensburg, Germany

MATERIALS AND METHODS

To determine whether residence in the ER that characterizes F508delCFTR can explain the difference in fracture pattern between wt-CFTR and the F508del mutant, we confined the wt-CFTR to the ER using the agent Brefeldin A that prevents budding from the ER to the Golgi as described previously for BHK cells[1].

Cells at 70 % confluence were treated with 100 μg/ml or 200 ng/ml Brefeldin A [1] for 2–8 h in complete medium with methotrexate as described in the Materials and methods section of the main text. Briefly, cells were washed with ice-cold PBS, scraped from the plates, pelleted by centrifugation and lysed by the addition of ice-cold buffer consisting of 1 % (v/v) Nonidet P40, 50 mM Tris/HCl (pH 7.5) and 150 mM NaCl, with fresh protease inhibitor cocktail (Calbiochem). Cells were lysed by incubation on ice for 20 min then the lysate cleared by centrifugation at 17000 ***g*** for 15 min at 4 °C. The supernatant was collected and subjected to a Bradford assay for protein concentration quantification.

Equal amounts of protein was loaded and analysed by SDS/PAGE and Western blotting as described in the Materials and methods section of the main text.

RESULTS

First, when CFTR synthesis was blocked with cycloheximide, for both wt-CTFR and F508delCFTR, 2 h was sufficient to attenuate band B (noting decreased band C for wt-CFTR, consistent with its slower turnover). Only for F508delCFTR was the cycloheximide inhibited, and a lower steady-state level of band B now at the limit of detection (Figure S1B, uppermost blots); unless the blots were overexposed (middle blots). Thus the relative decline in F508delCFTR was greater than for the wt consistent with the work of others showing a faster turnover for this mutant. However, despite this attenuation in fragment intensity, the fracture fingerprint was only marginally altered for wt-CFTR. For example, using the NBD2-directed antibody (left-hand panels), the region between 60 and 80 kDa was less intense when wt-CFTR synthesis was blocked. No statement can be made for F508delCFTR in this regard because the fragment fingerprints were below the limit of detection after synthetic block. Conversely, when ER escape was blocked by Brefeldin A, band B was increased in intensity (uppermost blots show two bands for wt-CFTR), but Brefeldin A does not alter the fingerprint (but can attenuate the fragment intensity after as little as 2 h of exposure). These combined data do suggest that neither prevention of entry nor elimination of exit from the ER can make the fingerprint pattern of wt-CFTR resemble F508delCFTR.

[1] These authors contributed equally to this work.
[2] To whom correspondence should be addressed (email a.mehta@dundee.ac.uk).

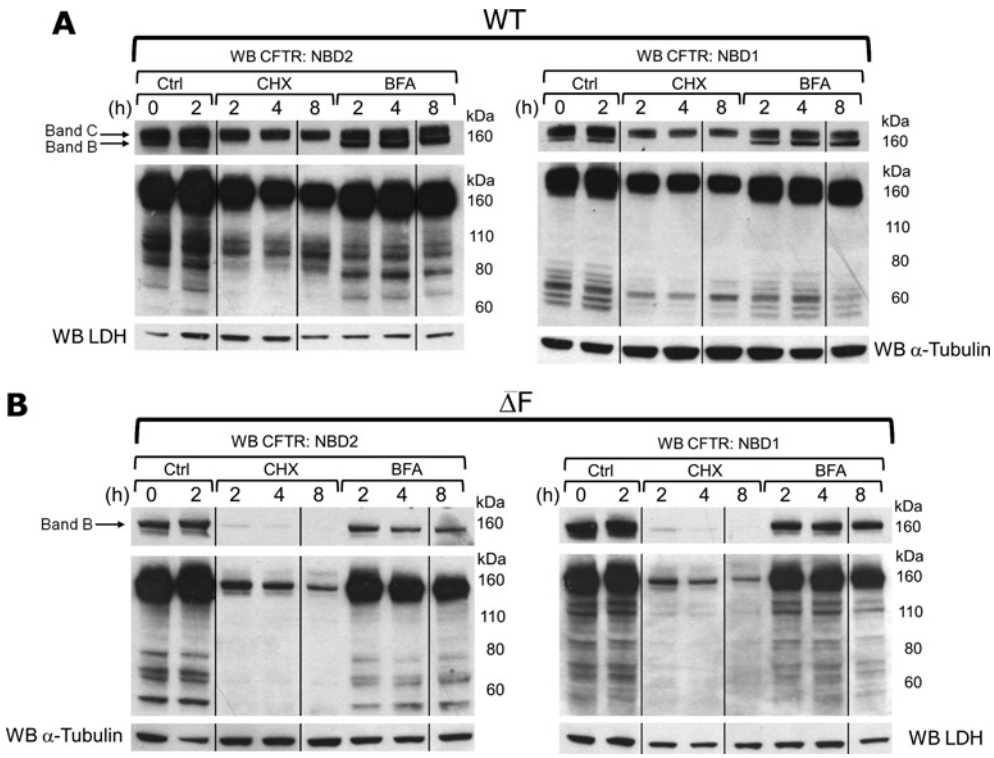

Figure S1 BHK cells expressing WT (A) or F508delCFTR (B) were exposed to either cycloheximide (CHX, 100 μg/ml) or Brefeldin A (BFA, 200 ng/ml) for up to 8 h (as indicated)

WT (15 μg) or F508delCFTR (ΔF; 20 μg) proteins were analysed with antibodies directed against NBD2 and NBD1. The middle Western blots shown are at higher exposures; the bottom blots are loading controls. The uppermost blots show full-length CFTR and reveal that CHX and BFA respectively attenuated or stabilized band B CFTR (160 kDa). The effect was more marked for F508delCFTR (**B**). The molecular mass in kDa is indicated on the right-hand side.

REFERENCE

1 Glozman, R., Okiyoneda, T., Mulvihill, C. M., Rini, J. M., Barriere, H. and Lukacs, G. L. (2009) N-glycans are direct determinants of CFTR folding and stability in secretory and endocytic membrane traffic. J. Cell Biol. **184**, 847–862

Received 3 August 2012/2 October 2012; accepted 15 October 2012
Published as BJ Immediate Publication 15 October 2012, doi:10.1042/BJ20121240